SUPPLEMENTARY MATERIALS

CO adsorption on pure, defective and mixed composition AlF_3 and MgF_2 surfaces – SUPPLEMENTARY MATERIALS

A. Impellizzeri [a]*, J. Dieu[b]*, J. Rousseau[b], S. Brunet[b]†, C. P. Ewels[a]†

1. Geometry and electronic properties of bulk MgF_2

In the present section we address the accuracy of different semi-local exchange correlation DFT functionals including the corrections of the vdW interactions for the bulk MgF_2 by comparison of the calculation results with the experimentally measurable quantities and literature values obtained using the same and higher level methods. Nonetheless, the geometry parameters of the rutile-like structure of MgF_2 are underestimated (overestimated) with LDA (GGA) methods tested here, the resulting GGA-PBE+D2 value (67.143 Å^3) are quite close with those obtained using the most reliable DFT-B3LYP hybrid functional (67.150 Å^3). In addition, the discrepancy for the calculated unit-cell volume between DFT-D2 method and the experiment is only 4.04% (reducing to 2.88% depending on the experimental literature value taken). All of these considerations are summarized in Table 1. The difference between our LDA values and those reported in the literature at the same level of approximation can be attributed, not to the functional choice, but to the basis set employed in the calculations. In fact, by reducing the number of basis functions from 40 (*dddd*) to 28 (*ddpp*) the new LDA values are: *a*, *b* = 4.92 Å and *c* = 2.55 Å with a total volume V = 61.73 Å^3, which is quite similar with that obtained in the work of Han et al.[1] (61.81 Å^3).

*Table S**1**. Lattice vectors (in Å) and calculated volumes (in Å^3) obtained using LDA and GGA-PBE implementing various versions of van der Waals corrections for bulk MgF_2. Literature experimental and theoretical values are also given for comparison.*

Method	*a*, *b* [Å]	*c* [Å]	V [Å^3]	ΔV [%]
Expt.[2,3]	4.60	3.05	64.538	0.00
Expt.[4]	4.615	3.043	64.810	+0.42
Expt.[5]	4.625	3.052	65.284	+1.16
Expt.[1]	4.621	3.052	65.171	+0.98
LDA[1,6]	4.539	3.000	61.808	-4.23
GGA-PBE	4.673	3.077	67.192	+4.11
B3PW	4.654	3.139	67.990	+5.35
B3LYP	4.667	3.083	67.150	+4.05
B3LYP	4.665	3.083	67.093	+3.96
LDA	4.477	2.957	59.269	-7.91
GGA-PBE	4.719	3.125	69.590	+7.83
GGA-PBE+D2	4.669	3.080	67.143	+4.04
GGA-PBE+D3	4.695	3.114	68.642	+6.36

The performance of our selected DFT methods is further tested by analysing the quasiparticle band structure. It is known that MgF_2 is an insulator, characterized by a wide direct band gap nearly ranging from 10.8-12.4 eV, as estimated in the experimental studies referred in the work of Mahida *et al.*[7]

The LDA and GGA-PBE calculations show a direct band gap equal to 7.38 and 7.21 eV, respectively. The inclusion of dispersive D2 correction increases the band gap up to 7.42 eV. Although LDA and GGA-PBE without and with vdW forces likely systematically underestimate the semiconducting band gap, our values are higher than those provided in the literature at the same level of theory.[3,7] Amongst tested approximations, the GGA-D2(3) provides the highest quasiparticle energy gap value.

*Table **S2**. GGA-D2 calculated lattice vectors (in Å) and relative energy (in meV) of 3D bulk MgF_2 by varying the k-point grids used for the structural optimization.*

k-point grid	*a*, *b* [Å]	*c* [Å]	ΔE_{tot} [meV]
4 × 4 × 4	4.669	3.072	2.295
8 × 8 × 8	4.669	3.080	0.282
12 × 12 × 12	4.669	3.080	0.034
16 × 16 × 16	4.669	3.080	0.000
20 × 20 × 20	4.669	3.080	0.000
24 × 24 × 24	4.669	3.080	0.000

2. Geometry and vibrational frequencies of CO and CO_2 molecules

As expected, the absolute values of the harmonic frequency are sensitive to the chosen method. In general, LDA underestimates the C—O bond length of 0.010 Å and of consequence the frequency position for the associated stretching mode is overestimated (2188 cm^{-1}) with respect to the experimental counterpart in gas phase (2143 cm^{-1}).

In contrast GGA-PBE without and with vdW interactions reproduces exactly the same bond length of the isolated gas phase CO molecule. The corresponding vibrational frequencies are slightly underestimated (2139 and 2137 cm^{-1}) in comparison to the experimental value. Although, the inclusion of vdW forces induces a downshift of 2 cm^{-1}, it can be considered a reliable theory level for this study.

Similarly for CO_2, while LDA correctly predicts the bond length, the associated frequency value (2423 cm^{-1}) is very overestimated, while GGA+D is again better (~2360 cm^{-1}), only 11 cm^{-1} above experiment (~2349 cm^{-1}).

*Table S**3**. Dependence of bond lengths (in Å) and harmonic frequencies (in cm^{-1}) of DFT functionals (LDA and GGA) and Grimme's corrections (D2 and D3) for the optimised CO and CO_2 molecules in gas phase. Experimental values are given for comparison.*

Method	C—O Bond Length [Å]	ν [cm^{-1}]	Δν [%]
CO			
Expt.[8]	1.135	2143	0.00
LDA	1.125	2188	+2.10
GGA-PBE	1.135	2139	-0.19
GGA-PBE+D2	1.135	2137	-0.28
GGA-PBE+D3	1.135	2137	-0.28
CO_2			
Expt.[9]	1.162	2349	0.00
Expt.	-	2349	0.00
LDA	1.161	2423	+3.15
GGA-PBE	1.171	2361	+0.51
GGA-PBE+D2	1.172	2360	+0.47
GGA-PBE+D3	1.172	2360	+0.47

Surprisingly, our computed GGA+D results are closer to the experimental value with respect to other literature values calculated using more advanced hybrid functional and several basis sets.[9] All of these considerations are summarized in Table S2.

3. Effect of slab thickness on calculated CO frequency and binding

We examine here the variation in CO bond length and frequency as a function of slab thickness, taking the MgF_2 (001) and (110) surfaces as our test cases. These show that even for the thinner slabs the system is already well converged, with variation in the CO frequency of only ±1-3cm^{-1}.

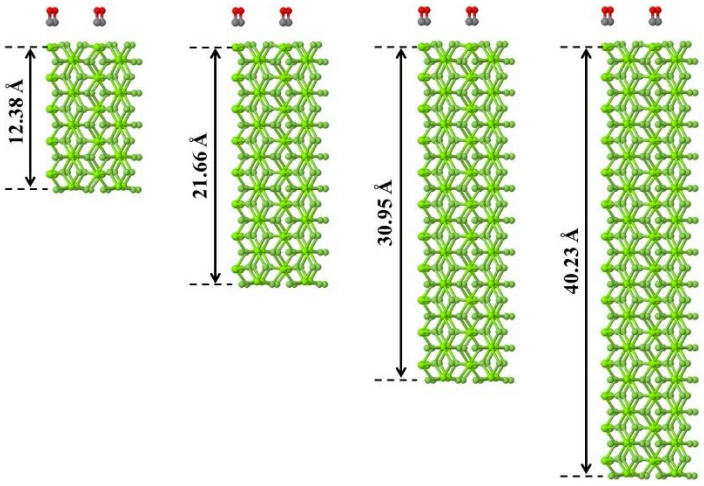

*Fig.S**1**. DFT-D2 optimized structures of CO molecule adsorbed above MgF_2 (001) surface with increasing slab thickness. Associated frequencies are given in Table S2.*

*Table **S4**. GGA-D2 calculated vibrational frequencies of CO molecules (cm^{-1}) adsorbed above MgF_2 (001) surface by increasing the slab thickness. The shaded box indicates the most stable binding site.*

	CO bonding site and orientation			
Slab Thickness [Å]	C above Mg [cm^{-1}]	O above Mg	C above F	O above F
12.38	2173	2131	2147	2191
21.66	2172	2131	2143	2190
30.95	2170	2131	2150	2190
40.23	2176	2130	2149	2191

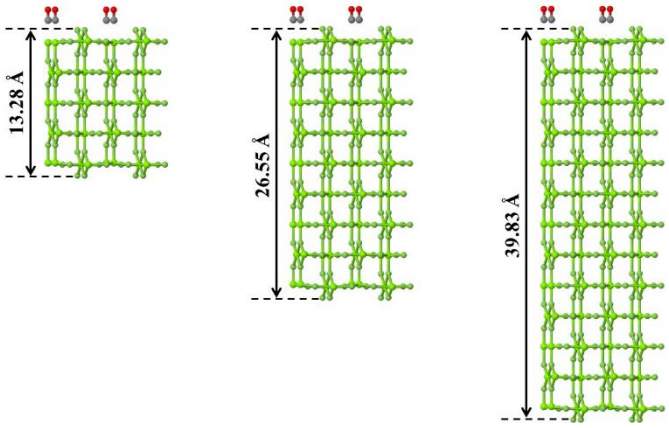

*Fig.S**2**. DFT-D2 optimized structures of CO molecule adsorbed above MgF_2 (110) surface with increasing slab thickness. Associated frequencies are listed in Table S4.*

*Table **S5**. GGA-D2 calculated vibrational frequencies of CO molecules (cm^{-1}) adsorbed above MgF_2 (110) surface by increasing the slab thickness. The shaded box indicates the most stable binding site.*

	CO bonding site and orientation		
Slab Thickness [Å]	C above Mg [cm^{-1}]	O above Mg	O above F
13.28	2189	2124	2089
26.55	2187	2125	2092
39.83	2187	2127	2092

4. Relative Energy and frequency of CO absorption at different surface sites on MgF_2.

The following figures show the relative energies of CO, varying the location and orientation on different surface facets of MgF_2. Numbers beneath each structure show its energy relative to the most stable at 0.00eV. Calculated frequencies (cm^{-1}) are shown above, and to take into account the shift with respect to experiment, we also quote the shift between the calculated value and that calculated for an isolated gas phase CO at the same level of theory (in brackets). Most stable structure is shown in a pale blue square each time. In each case this is with the C atom of CO closer to the surface, closest to an exposed Mg atom.

(a) CO on stable (110) MgF_2 surface (48cm^{-1} upshift in frequency):

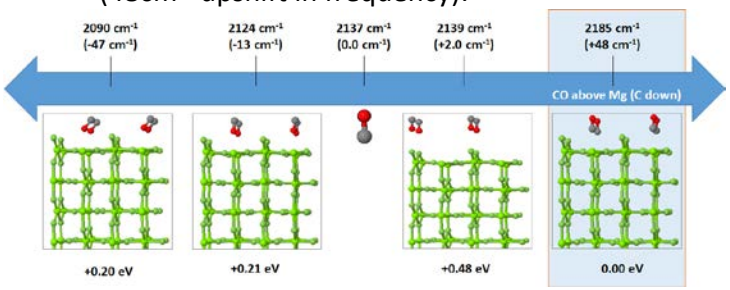

(b) CO on the less stable (101) MgF_2 surface (25cm^{-1} upshift):

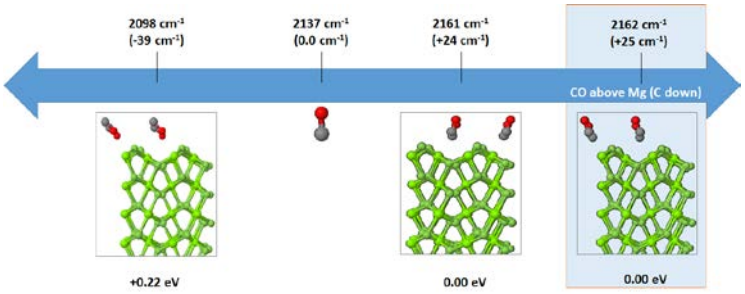

(c) CO on unstable (100) MgF_2 surface (31 cm^{-1} upshift):

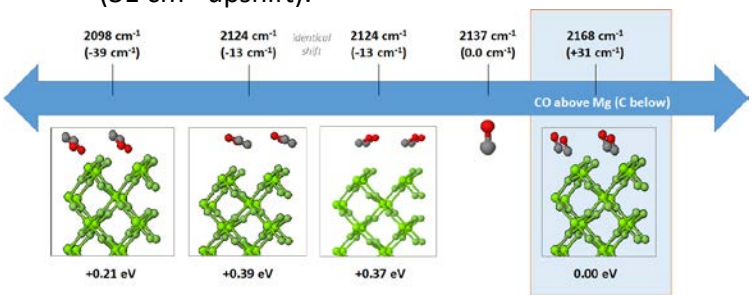

(d) CO on highly unstable (001) MgF_2 surface (10 / 34cm^{-1} upshift):

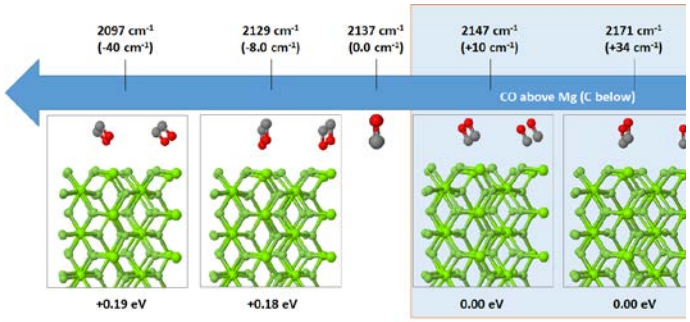

*Fig.S**3**. Calculated CO binding on different MgF_2 facets with relative binding energies (eV) compared to the most stable configuration, and calculated CO stretch frequency (cm^{-1}). The bracketed frequency is given relative to isolated gas phase CO.*

5. TEM of AlF_3 support without Mg treatment.

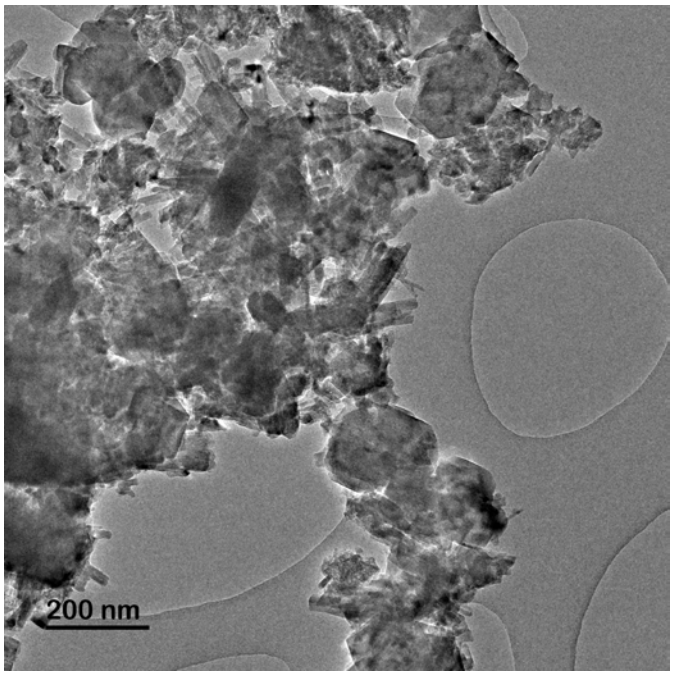

*Fig.S**4**. TEM of AlF_3 support without Mg treatment. The overall crystalline morphology is very similar to the 2 wt% Mg treated sample shown in the main paper.*

6. Experimental XRD data.

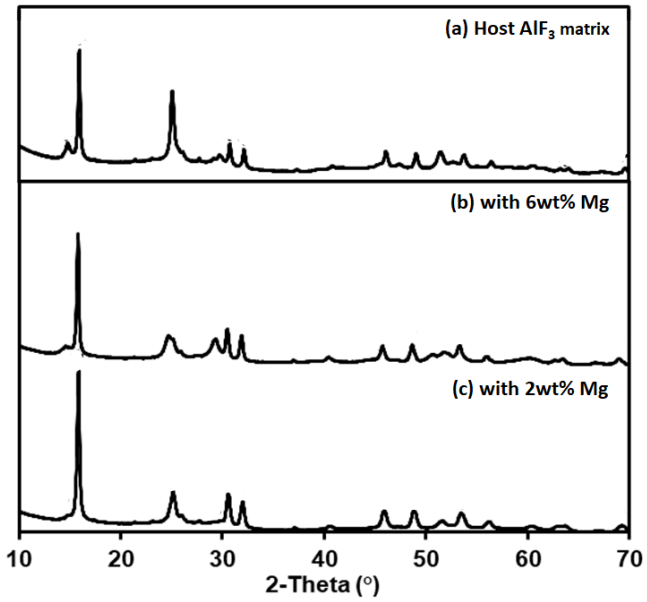

*Fig.S**5**. XRD data of the samples (a) the original support structure (AlF_3) and (b,c) with 6 and 2wt% Mg deposition respectively. While the peaks show the relatively high crystallinity of the samples, precise peak assignment is difficult given the sample synthesis (sample cores of alumina, with stabilised fluorinated surface layers)*

References

1 H. Han, G. Yin, H. Wang, C. Wang, K. Shao, W. Zhang, J. Dai and P. Huai, *Computational Materials Science*, 2017, **133**, 159–166.

2 M. Catti, A. Pavese, R. Dovesi, C. Roetti and M. Causà, *Phys. Rev. B*, 1991, **44**, 3509–3517.

3 Z. Yi and R. Jia, *Journal of Physics: Condensed Matter*, 2012, **24**, 085602.

4 A. F. Vassilyeva, R. I. Eglitis, E. A. Kotomin and A. K. Dauletbekova, *Central European Journal of Physics*, 2011, **9**, 515–518.

5 W. H. Baur, *Acta Crystallographica*, 1956, **9**, 515–520.

6 Z. Huesges, C. Müller, B. Paulus, C. Hough, N. Harrison and E. Kemnitz, *Surface Science*, 2013, **609**, 73–77.

7 H. R. Mahida, D. Singh, Y. Sonvane, S. K. Gupta and P. B. Thakor, *Solid State Communications*, 2017, **252**, 22–28.

8 S. C. Street, C. Xu and D. W. Goodman, *Annual Review of Physical Chemistry*, 1997, **48**, 43–68.

9 E. J. Berquist, C. A. Daly, T. Brinzer, K. K. Bullard, Z. M. Campbell, S. A. Corcelli, S. Garrett-Roe and D. S. Lambrecht, *The Journal of Physical Chemistry B*, 2017, **121**, 208–220.